Journal of Histochemistry & Cytochemistry 2016, Vol. 64(7) 441–453

DOI: 10.1369/0022155416652611
jhc.sagepub.com
SAGE

Periostin Deficiency Causes Severe and Lethal Lung Injury in Mice With Bleomycin Administration

Hirofumi Kondoh, Takashi Nishiyama, Yoshinao Kikuchi[†], Masashi Fukayama, Mitsuru Saito, Isao Kii[*], and Akira Kudo[*]

Department of Biological Information, Graduate School of Bioscience and Biotechnology, Tokyo Institute of Technology, Yokohama, Japan (HK, TN, IK, AK); Department of Pathology, Graduate School of Medicine, University of Tokyo, Tokyo, Japan (YK, MF); Department of Orthopaedic Surgery, Jikei University School of Medicine, Tokyo, Japan (MS); and Pathophysiological and Health Science Team, Imaging Application Group, Division of Bio-Function Dynamics Imaging, RIKEN Center for Life Science Technologies, Kobe, Japan (IK)

Summary

Pulmonary capillary leakage followed by influx of blood fluid into the air space of lung alveoli is a crucial step in the progression of acute lung injury (ALI). This influx is due to increased permeability of the alveolar–capillary barrier. The extracellular matrix (ECM) between the capillary and the epithelium would be expected to be involved in prevention of the influx; however, the role of the ECM remains to be addressed. Here, we show that the ECM architecture organized by periostin, a matricellular protein, plays a pivotal role in the survival of bleomycin-exposed mice. Periostin was localized in the alveolar walls. Although periostin-null mice displayed no significant difference in lung histology and air–blood permeability, they exhibited early lethality in a model of bleomycin-induced lung injury, compared with their wild-type counterparts. This early lethality may have been due to increased pulmonary leakage of blood fluid into the air space in the bleomycin-exposed periostin-null mice. These results suggest that periostin in the ECM architecture prevents pulmonary leakage of blood fluid, thus increasing the survival rate in mice with ALI. Thus, this study provides an evidence for the protective role of the ECM architecture in the lung alveoli. (J Histochem Cytochem 64:441–453, 2016)

Keywords

acute lung injury, alveolus, bleomycin, collagen, extracellular matrix, fibronectin, matricellular, periostin, pulmonary leakage, stroma

Introduction

Acute lung injury (ALI) causes acute respiratory distress syndrome (ARDS), followed by pulmonary fibrosis (PF), and is regarded as a devastating pathological condition with a mortality rate of 30% to 40%.[1] ALI is characterized by increased permeability and influx of blood fluid into the air spaces, which impairs the pulmonary gas exchange, leading to arterial hypoxemia and respiratory failure.[1] PF is a chronic and progressive disease associated with fibrotic lung disorder.[2] PF is characterized by excessive accumulation of extracellular matrix (ECM) proteins such as interstitial collagen, fibronectin, and proteoglycans expressed in fibroblasts activated by TGF-β.[3–5] Recent detailed studies indicated that PF is

*These authors contributed equally.

[†]Presently at Department of Pathology, Teikyo University School of Medicine, 2-11-1 Kaga, Itabashi-ku, Tokyo 173-8605, Japan.

Received for publication December 3, 2015; accepted May 10, 2016.

Corresponding Author:
Isao Kii, Pathophysiological and Health Science Team, Imaging Application Group, Division of Bio-Function Dynamics Imaging, RIKEN Center for Life Science Technologies, 6-7-3 Minatojima-minamimachi, Chūō-ku, Kobe, Hyogo 650-0047, Japan.
E-mail: isao.kii@riken.jp

Journal of Histochemistry and Cytochemistry

dramatically improved by deletion of the periostin gene, coding for a matricellular protein, expressed in the activated fibroblasts in a mouse model with administration of bleomycin (10 mg/kg body weight).[6] This treatment causes more than 80% lethality for wild-type BALB/c mice, which exhibit a bleomycin resistance and a PF.[7] Interestingly, another group demonstrated that inhibition of periostin with anti-periostin antibody also improves bleomycin-induced PF.[8] These data indicate that periostin exacerbates fibrosis in the bleomycin-induced PF model.

Periostin is involved in construction of the ECM architecture.[9–14] This protein is expressed in normal and pathological connective tissue,[15] for example, periosteum, periodontal ligament, aorta, cardiac valve,[16–19] developing heart,[20] cardiac hypertrophy,[21] granulation tissue in myocardial infarction,[11] cutaneous excisional wound,[14] and tumor stroma,[11,14,20–24] all of which are constantly subjected to mechanical stress. Especially, the maximum rupture pressure in the infarcted myocardium is significantly lower in periostin-null mice than in wild-type mice,[11] indicating that the infarcted myocardial wall of periostin-null mice is susceptible to mechanical stress.

Lung alveoli are also subjected to mechanical stress during respiration and pulmonary blood flow. Especially, when damaged by ALI, alveolar walls are considered sensitive to mechanical stress.[25,26] Type I collagen is detected in the alveolar wall[27] and is the most dominant component responsible for the mechanical strength of lung ECMs.[28] Collagen fibrillogenesis is stabilized by the cross-linking activity of lysyl oxidase (LOX).[29] The LOX enzymatic activity is regulated by periostin via bone morphogenetic protein 1 (BMP-1) activation,[30] and it has been revealed that periostin plays a role in covalent cross-linking between collagen fibrils in the infarcted myocardium and the bone.[11,12,30] Moreover, periostin regulates the amount of collagen in tissue.[10,11] Taken together, these reports indicate that periostin is responsible for the amount of tissue collagen and fibrillogenesis, which underlie ECM strength. Our preliminary study and another group demonstrated that periostin is expressed during lung development and is localized in intact alveolar wall.[31] However, the role of periostin in the intact lung remains elusive.

In this present study, we investigated whether periostin plays a role especially in the ALI phase that occurs immediately after bleomycin administration. To induce ALI in mice as an animal model, intratracheal administration of bleomycin is often used.[32] This model induces a series of symptoms: ALI, lung inflammation, and PF. We induced lung injury in mice with C57BL/6 background, which are more sensitive to bleomycin than BALB/c mice. The mice were given a single injection of 2.5 U/kg of bleomycin in the survival study or a single injection of 5 U/kg in the histological analysis. The reason why we selected 2.5 U/kg in the survival assay is to prevent death caused by PF in wild-type mice as possible. In contrast, we exposed mice with 5 U/kg in histological analysis to distinguish alveolar damages. The bleomycin-administered periostin-null mice exhibited a higher rate of lethality than their wild-type counterparts, suggesting a protective role of periostin in ALI.

Materials and Methods

Mice and Bleomycin Treatment to Induce ALI

Care and experiments with animals were in accordance with the guidelines of the animal care and use committees at Tokyo Institute of Technology. Generation and maintenance of periostin-null mice were described previously.[11] Eight-week-old C57BL/6 background periostin-null and wild-type mice were treated with a single dose of 2.5 or 5.0 U/kg body weight of bleomycin sulfate (LKT Laboratories, Inc., St. Paul, MN; 2.5 U/kg for survival rate, 5.0 U/kg for pathological analysis) by intratracheal injection in a total volume of 18 to 34 µl of saline under anesthesia achieved with an intraperitoneal injection of Nembutal (Dainippon Pharmaceutical Co., Ltd., Osaka, Japan).

RT-PCR Analysis

The lung tissues from 8-week-old wild-type mice were immersed in ISOGEN (Wako Pure Chemical Industries, Ltd., Osaka, Japan). Total RNA was extracted and subjected to reverse transcription by using a first-strand cDNA synthesis kit (Life Sciences, Inc., St. Petersburg, FL). To identify the alternatively spliced variant forms, we used the specific primers for each variant form as described previously.[11] cDNA corresponding to each variant form was amplified with Ex Taq DNA polymerase (Takara Bio, Inc., Otsu, Japan). PCR parameters were as follows: initial denaturation at 95C for 3 min followed by 26 cycles of denaturation at 95C for 1 min, and annealing and extension at 68C for 1 min, and a final extension at 72C for 2 min. The amplified DNA bands were confirmed by 1.5% agarose gel electrophoresis.

Western Blot

The lung tissues excised from 8-week-old wild-type and periostin-null mice were immersed in SDS sample buffer, pulverized with a handy sonicator (ULTRA5

Homogenizer, VP-55, TIETECH Co., Ltd., Nagoya, Japan) and then heated at 95C for 5 min with dithiothreitol (DTT) at a final concentration of 10 mM. Lung tissue extracts were separated by SDS-PAGE on 10% acrylamide gels and electroblotted onto Immobilon-P membranes (Millipore Corporation, Billerica, MA) for detection of periostin. Antibodies against mouse periostin (rabbit polyclonal anti-CT and rabbit polyclonal anti-RD1, raised in our laboratory; 1:2000[12]) were used as primary antibodies. Bound primary antibodies were detected with horseradish peroxidase (HRP)–conjugated secondary antibodies and Immobilon Western Chemiluminescent HRP Substrate (Millipore).

Immunohistochemistry

Adult mouse lungs (from 8-week-old mice) were perfused, inflated with 50-mM EDTA/PBS, excised, and fixed in 4% paraformaldehyde in PBS at 4C overnight. Subsequently, the lungs were embedded in Tissue-Tek O.C.T Compound (Sakura Finetek Japan Co., Ltd., Tokyo, Japan) for frozen blocks or Pathoprep 568 (Wako) for paraffin blocks, and 4-μm sections were collected and processed for immunostaining. Antibody against mouse periostin (rabbit polyclonal anti-RD1, 1:200) was described previously.[11] Rabbit polyclonal anti-mouse fibronectin antibody (Ab-10; 1:100) was obtained from NeoMarkers (Fremont, CA). For general immunostaining, slides were rehydrated and incubated at 4C overnight with the primary antibody without antigen retrieval. HRP-conjugated secondary antibodies (Envision+ Signal Reagent; Dako, Glostrup, Denmark) and the HRP detection kit (Liquid DAB+ Substrate; Dako) were used for signal visualization. To detect mouse periostin and fibronectin, we applied anti-RD1 on paraffin sections and Ab-10 on cryosections, respectively. For negative controls, we applied an equal molar of rabbit IgG.

In Vivo Pulmonary Permeability Assay

Lung permeability was measured with Evans blue dye (Sigma-Aldrich, St. Louis, MO) by using a previously described technique.[33] Briefly, 8-week-old mice were injected intravenously with Evans blue dye (20 mg/kg). Three hours later, they were sacrificed and perfused with PBS to remove excess dye and blood cells from the lungs. Thereafter, the lung tissue was collected and homogenized. The Evans blue dye was extracted with formamide during overnight incubation at 60C followed by centrifugation at 5000 × g for 30 min. The concentration of the dye was determined based on the absorption at 620 and 740 nm.

Quantification of Collagen Contents and Cross-Linkages

The concentrations of collagen and pyridinoline in the lung were used for the quantitative analysis by high-performance liquid chromatography (HPLC) using a fluorescence detection method established previously.[34] Sample preparation for HPLC was as follows: The lungs from 19-week-old and 35- to 36-week-old mice were snap-frozen, and pulverized in liquid nitrogen. All tissues were suspended and stirred in 50-mM potassium phosphate buffer (pH 7.6) at 4C for 72 hr under a vacuum, and then a 1/30 volume of sodium borohydride ($NaBH_4$) was added to the solution. The reaction was allowed to proceed for 60 min at 37C and was terminated by the addition of 3-N acetic acid to decrease the pH value to 4.0. The solution residue was collected by centrifugation (3000 × g, 15 min), washed with deionized water, and lyophilized. For HPLC analysis, lyophilized samples were dissolved in 0.2-N sodium citrate buffer (pH 2.2) and filtered through a 0.45-μm filter (Gelman Science Japan Ltd., Tokyo, Japan). The analysis of enzymatic mature pyridinium cross-links, such as pyridinoline (PYD), was performed on a single-column HPLC. Hydrolysates were analyzed for pyridinoline and hydroxyproline levels on a Shimadzu LC9 HPLC fitted with a cation exchange column (0.9 × 10 cm, Aa pack-Na; JASCO, Ltd., Tokyo, Japan). It was assumed that collagen weighed 7.5 times the measured weight of hydroxyproline, with a molecular weight of 300,000 Da.[34] The resulting data were used to calculate cross-link values as mol/mol of collagen.

Transmission Electron Microscopy

The lungs of 11-week-old wild-type and periostin-null mice were expanded with 70 μl of PBS, perfused with 4% paraformaldehyde (TAAB Laboratories Equipment, Ltd., Berks, UK), and fixed in 2.5% glutaraldehyde/4% paraformaldehyde. Subsequently, the lungs were fixed with 1% osmium tetroxide in PBS. Specimens were embedded in Quetol 812 (Nisshin EM Co., Ltd., Tokyo, Japan), sectioned at 80 nm by using an Ultracut UCT ultramicrotome (Leica Microsystems, Inc., Bannockburn, IL), and stained with 1.2% tannic acid, 2% uranyl acetate, and 0.5% lead citrate. Stained ultrathin sections were viewed with a Hitachi H7500 transmission electron microscope (Hitachi, Ltd., Tokyo, Japan) operated at 80 kV.

Measurement of Protein Concentration in Bronchoalveolar Lavage Fluid (BALF)

To measure protein leakage in the bleomycin-exposed lung, bronchoalveolar lavage was performed (500 μl of

PBS given 2 times) at day 5 after bleomycin administration. In each mouse, 80% (800 µl) of the total injected volume was consistently recovered. The BALF was centrifuged at 1500 rpm for 10 min and then at 15,000 rpm 2 times for 10 min each time. The final supernatants were utilized for measurement of protein concentration determined with CBB (Coomassie Brilliant Blue; Nacalai Tesque, Inc., Kyoto, Japan). The CBB protein assay was performed on serial dilutions of the supernatant. Ten minutes after having mixed the supernatant and CBB solution, the absorbance values at 595 nm were measured in a 96-well protein assay plate by using a Bio-Rad Model 550 microplate reader (Bio-Rad Laboratories, Inc., Hercules, CA) with a BSA dilution series used for preparation of a standard curve. The concentrations were calculated from the absorbance, and the ratio between the wild-type and the periostin-null BALF was estimated for each lot of bleomycin.

Statistics

To assess differences among groups, we performed statistical analysis with the log-rank test for the survival rate and the Mann–Whitney *U* test for the others, using Prism 6.0 (GraphPad Software, Inc., San Diego, CA). The results were shown as the mean ± SD) with *p* values (*$p<0.05$, **$p<0.01$).

Results

Expression of Periostin in Mouse Lung

To examine whether periostin was expressed in lung tissue, we investigated the periostin transcripts in the mouse lungs. Periostin transcripts in the periodontal ligament[35] and infarcted myocardium[11] consist of several alternatively spliced variant forms of its carboxyl terminal region. Four alternatively spliced variants, that is, full (full length), Δb (deletion of exon b), Δe (deletion of exon e), and ΔbΔe (deletion of exons b and e), were examined, and one specific spliced form, ΔbΔe, was dominantly detected (Fig. 1A and B).

To confirm the expression of periostin protein, we prepared tissue lysates from mouse lungs, which were then subjected to SDS-PAGE followed by Western blot analysis using anti-periostin antibodies (anti-CT and anti-RD1). We found one major band recognized by the anti-CT antibody, and three major ones recognized by the anti-RD1 antibody (Fig. 1A and C). The sizes of these three bands were approximately 90, 84, and 74 kDa. The 90-kDa band corresponded to the intact periostin protein, and the 84- and 74-kDa bands corresponded to the cleaved forms of periostin, which were reported previously.[11,12]

To investigate the localization of periostin protein in the lungs, we stained paraffin sections of the mouse lung with anti-RD1 antibody. Histological sections of the lung tissue showed alveoli composed of type I and II pneumocytes and capillary vessels (Fig. 1C). Immunoreactivity for periostin was detected in the alveolar walls (Fig. 1D).

Histological Analysis of Lung Tissue From Periostin-Null Mice

To elucidate the role of periostin in lung homeostasis, we performed histological analysis of lung tissue from periostin-null mice. Periostin-null mice are born alive and develop in a manner indistinguishable from that of their wild-type littermates except for the disturbed eruption of incisors.[17] Histological sections showed no apparent disorder in the periostin-null alveolar structure compared with that in the wild-type counterpart (Fig. 2A). Type I and II pneumocytes, as well as the alveolar walls, appeared intact in the periostin-null alveoli, as in the wild-type ones. The same was shown in 60-week-old mice (data not shown). We then examined fibronectin; however, no significant difference in immunoreactivity for fibronectin between wild-type and periostin-null alveoli was observed (Fig. 2B).

To further investigate the ECM architecture, we measured pulmonary permeability by using the Evans blue dye extravasation assay. The blue coloration of the tested lungs did not show any significant difference (Fig. 2C), indicating that the absence of periostin did not affect the intact lung structure or air–blood barrier.

Quantification of Collagen Content and Cross-Linkages in the Intact Lungs

The collagen amount and fibrillogenesis are responsible for the tensile strength of the lung ECM.[28] Periostin is known to be involved in both collagen amounts and cross-linkage.[10–12,30] Hence, we quantified these parameters in the intact lungs of wild-type and periostin-null mice. In the 19-week-old mice, the collagen content (percentage of tissue dry weight) tended to be less in the periostin-null mice than in the wild-type mice (0.79-fold less in periostin-null mice), and collagen cross-linkage assessed by the amount of pyridinoline (cross-linked peptide) per mole of collagen also tended to be less in these periostin-null mice (0.89-fold less in periostin-null mice, Fig. 3A), although both results showed no statistical difference. In the 35- to 36-week-old mice, the collagen content and the cross-linkage were not so different from those in the 19-week-old mice (collagen contents: 0.84-fold in periostin-null mice, $p=0.0095$; cross-linkages: 0.87-fold in periostin-null mice, $p=0.0095$; Fig. 3B). These data indicate

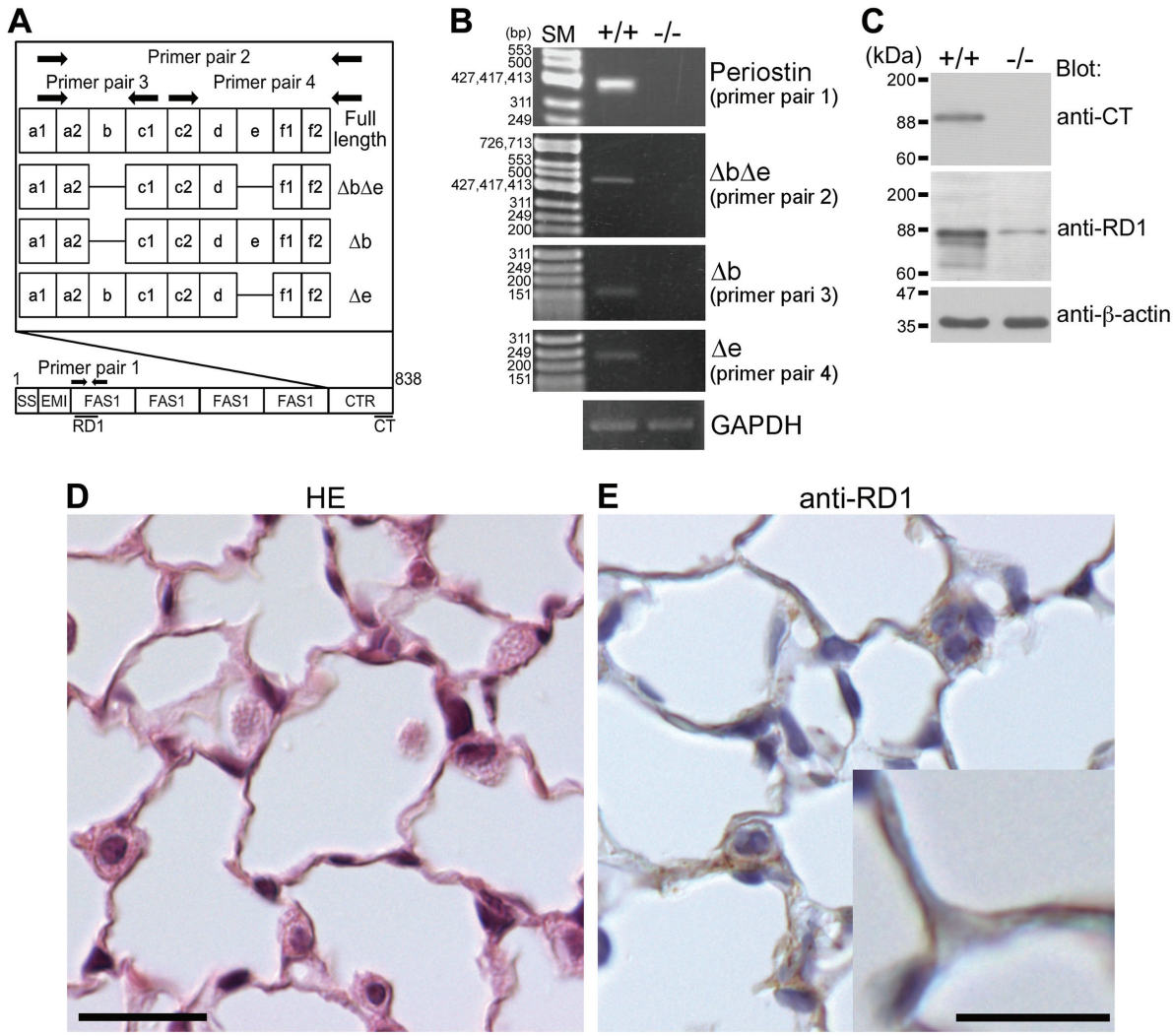

Figure 1. Expression of periostin in the lungs of wild-type mice. (A) Pattern diagrams of the periostin splice variant forms, primer pairs, and antibody recognition sites. SS, EMI, FAS1, and CTR mean signal sequence, EMI (EMILIN) domain, Fasciclin 1 domain, and C-terminal region, respectively. Periostin antibody recognition sites are indicated as black lines. (B) Expression of the periostin alternatively spliced variant form ΔbΔe in lung tissue from 8-week-old wild-type mice. Details on the primer pairs 1, 2, and 3 are described in the "Materials and Methods" section. GAPDH is shown as an internal control. +/+ indicates wild type and −/− indicates negative control (periostin-null mouse). SM means size marker. (C) Expression of periostin protein in lung tissue. Tissue lysates from the lungs of 8-week-old wild-type and periostin-null mice were subjected to SDS-PAGE. Proteins were visualized by blotting with anti-CT, anti-RD1, and anti-β-actin antibodies. A band corresponding to intact periostin is located at the 90-kDa position and those of cleaved periostin at approximately 84 and 74 kDa. +/+ indicates wild type and −/− indicates negative control from periostin-null mouse. The band located at the 90-kDa position in the −/− lane indicates a nonspecific signal. (D) Histological section of a lung alveolus of an 8-week-old wild-type mouse. The paraffin section was stained with hematoxylin–eosin (HE). (E) Localization of periostin protein in a lung alveolus from an 8-week-old wild-type mouse. The paraffin section was stained with anti-RD1 antibody, which was then counterstained with hematoxylin. Periostin is localized in the alveolar walls and in type II pneumocytes. Scale D = 20 μm; Scale E = 20 μm (high magnification = 10 μm).

that periostin was responsible for collagen synthesis and fibrillogenesis in the mouse lung tissue.

Ultrastructural Analysis of Lung Alveoli by Transmission Electron Microscopy

Next, we analyzed the microstructure of the lung alveoli by using transmission electron microscopy (TEM). Both wild-type and periostin-null alveoli were composed of type I and II pneumocytes and several capillary vessels without any obvious difference in their contour (Fig. 2A). Type I pneumocytes in the periostin-null alveoli, which cells are the main component of the alveolar wall, appeared almost the same in shape, size, and number as in the wild-type alveoli (Fig. 4A and B). The distribution of capillary vessels and the thickness of

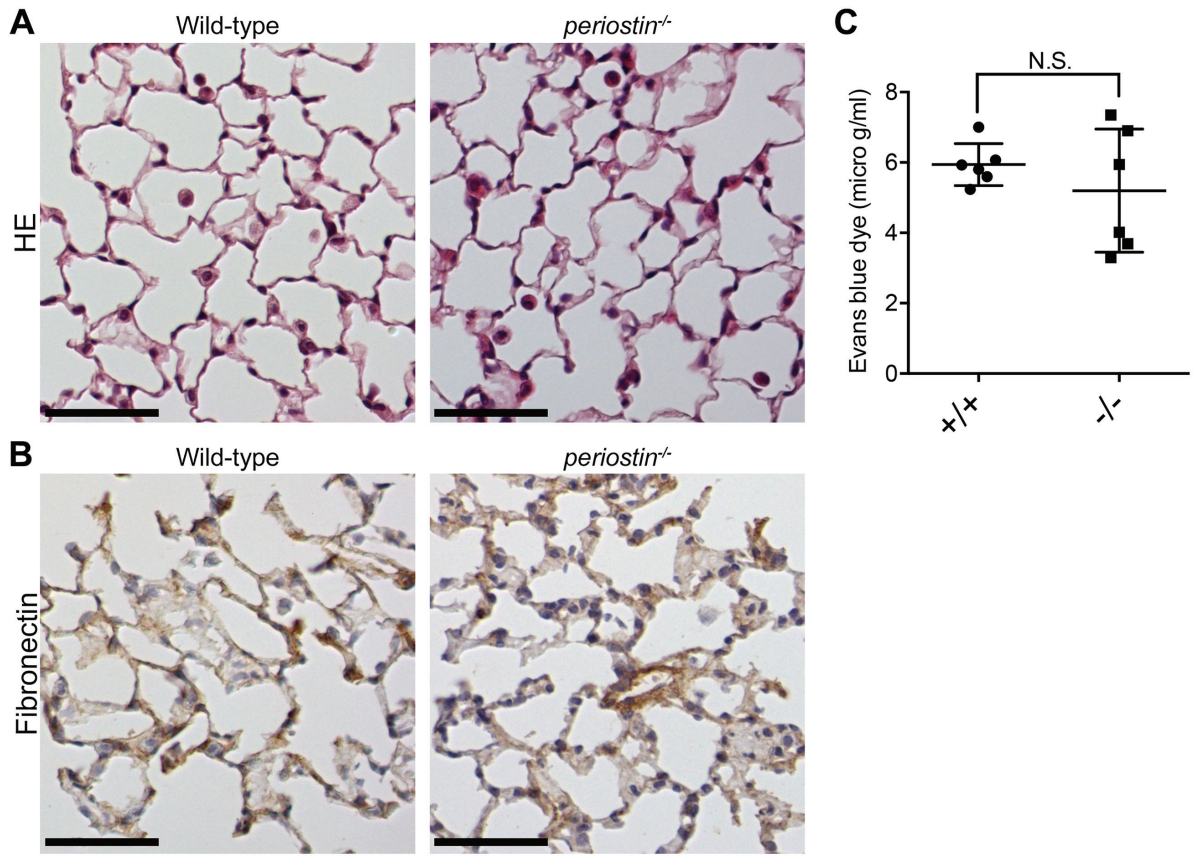

Figure 2. Lung histology for wild-type and periostin-null mice. (A) Histological sections of lungs from 8-week-old wild-type and periostin-null mice. The paraffin sections were stained with hematoxylin–eosin. (B) Detection of fibronectin in lungs from wild-type and periostin-null mice. Frozen sections of lungs from 8-week-old wild-type and periostin-null mice were stained with antifibronectin antibody, which were then counterstained with hematoxylin. (C) Vascular permeability of intact mouse lung. Vascular permeability was measured in terms of Evans blue dye leakage into the lungs of 8-week-old wild-type (+/+; *n*=6) and periostin-null (−/−; *n*=6) mice. Error bars represent the mean ± SD. N.S. means no significant difference. Scale A = 50 μm; Scale B = 50 μm.

vessel walls exhibited no difference between wild-type and periostin-null alveoli (Fig. 4A and B). To examine the architecture of the pulmonary cells in the alveoli of wild-type and null mice, we focused on the collagen fibrils seen in highly magnified images and found no significant difference in the fibril amount, shape, or diameter between wild-type and periostin-null alveolar walls (Fig. 4A–F). Despite the constant expression of periostin in the lungs of wild-type mice and difference in the amounts of collagen and cross-linkages, the intact lungs of periostin-null mice did not have any microstructural disorder.

Rate of Lethality Caused by Bleomycin Administration Was Higher in Periostin-null Mice Than in Their Wild-type Counterparts

To test the mechanical strength of the ECM in the alveoli, we administered bleomycin that rarely causes lethal ALI and PF in wild-type mice,[36] but does induce ECM fragility.[25,26] We first examined the survival rate of the 2.5 U/kg of bleomycin-exposed wild-type and periostin-null mice. Periostin-null mice began to die at day 7.5 after the bleomycin administration, though their wild-type counterparts started to do so later at day 12.5 (Fig. 5A). Both wild-type and periostin-null mice continued to die; however, the lethality of the periostin-null mice was greater than that of the wild-type mice. At day 20.5, the survival rate of periostin-null mice was 55% compared with the 83% for the wild-type ones (Fig. 5A). These results suggest that the bleomycin administration caused greater damage in the lung tissue of periostin-null mice than in that of the wild-type mice.

To investigate the damage in the bleomycin-exposed periostin-null lung tissue, we conducted histological analysis of the 5.0 U/kg of bleomycin-exposed lung. At 7 days after bleomycin administration, the

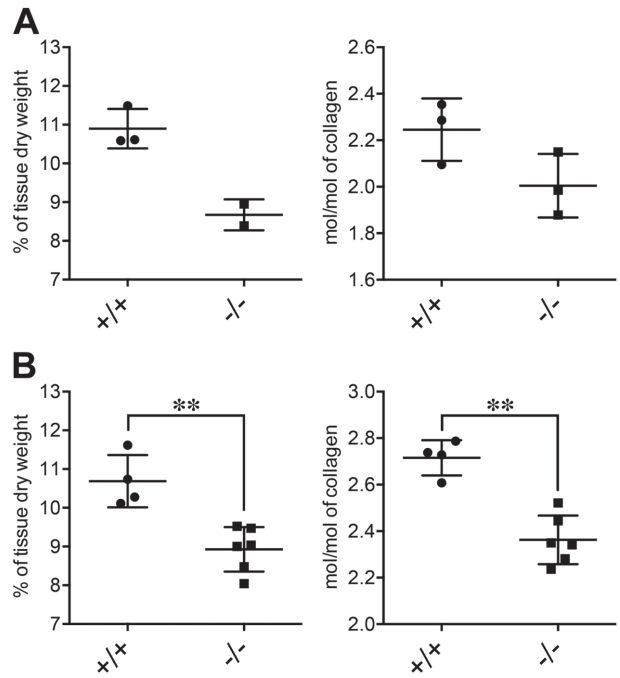

Figure 3. Collagen content and collagen cross-linkage in lungs of wild-type and periostin-null mice. (A) Collagen contents (percentage of tissue dry weight) and pyridinoline (PYD) contents (mol/mol of collagen) for 19-week-old wild-type (+/+; *n*=3) and periostin-null (−/−; *n*=2 for collagen content and *n*=3 for PYD contents) mice. (B) Same type of data for 35- to 36-week-old wild-type (+/+; *n*=4) and periostin-null (−/−; *n*=6) mice. Statistical significance of differences: $^{**}p<0.01$ as indicated by the brackets ($p=0.0095$ in each analysis of B).

alveolar interstitium of the wild-type mice was slightly thickened, but not in the case of the periostin-null counterpart (Fig. 5B). This result is compatible with that of a previous study.[6] However, the hemorrhagic edema with leakage of blood fluid into the air spaces of the alveoli was prominent in the periostin-null lungs, whereas the leakage was rarely observed in the wild-type ones (Fig. 5B). To quantify the leakage of blood fluid into the air spaces, we measured the erythrocyte concentration in the air spaces. At day 7 after the bleomycin administration, the erythrocyte concentration in the lungs from periostin-null mice was over 2-fold higher than that in those of the wild-type animals (Fig. 5C). The total protein in BALF at day 5 after bleomycin administration was also measured. The protein content in the periostin-null BALF was 1.5-fold higher than that for the wild-type one (Fig. 5D). These results indicate that the bleomycin administration induced more severe ALI in the periostin-null mice and that the difference between wild-type and periostin-null mice appeared at an early stage after bleomycin administration.

Discussion

This study demonstrated that mice lacking their periostin gene exhibited early lethality with elevated alveolar–capillary permeability and alveolar rupture in the resulting ALI-like model, in which the C57BL/6 background mice were administrated with bleomycin at the dose that did not cause severe lethality in wild-type mice. Several groups have reported that periostin exacerbates lethal PF and that deletion of the periostin gene in mice[6] or injection of periostin-neutralizing antibody (OC-20) during fibrosis progression alleviates this symptom.[6,8] The mouse strain, material, methodological, and phenotypical differences between the two studies and ours were described in Table 1. These two previous reports indicated a role for newly expressed periostin in the activated fibroblasts. Uchida et al.[6] demonstrated that 10 mg/kg of bleomycin induces severe PF in BALB/c background mice. Wild-type mice begin to die at 1 week after the bleomycin administration and show more than 80% mortality at 4 weeks.[6] In contrast, bleomycin-administered periostin-null mice exhibit mild fibrosis and lethality (10%).[6] Because periostin is expressed in intact lung alveoli, the role of which remains elusive, we examined the role of periostin in the alveolar wall ECM with bleomycin at the dose that did not induce lethal fibrosis in wild-type mice. Lung cells of BALB/c mice are more resistant to bleomycin than those of C57BL/6 mice because of the high expression of a bleomycin-detoxifying enzyme, bleomycin hydrolase,[7] and the high rate

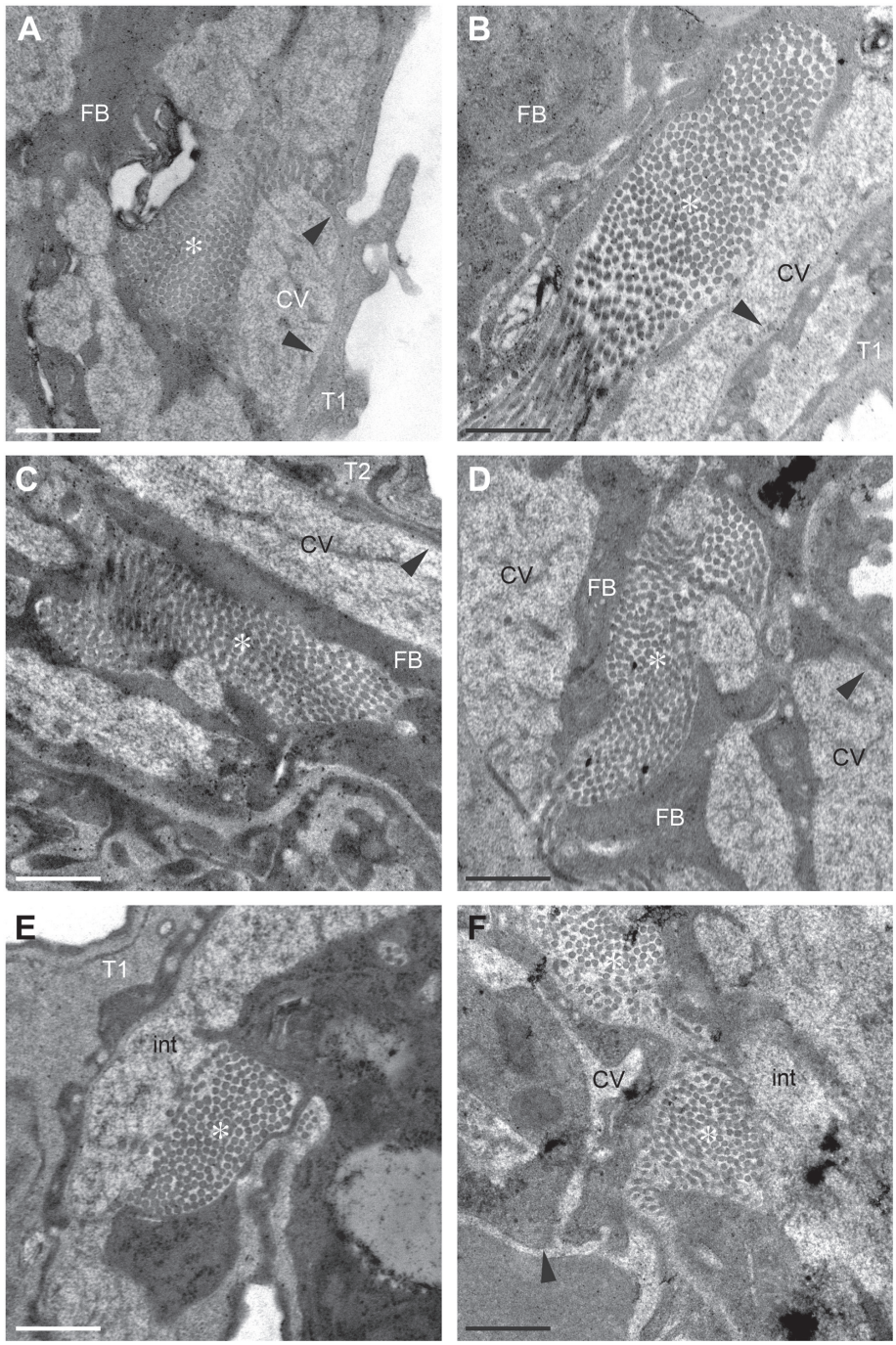

Figure 4. Transmission electron microscopy (TEM) analysis of wild-type and periostin-null lung tissue. (A–E) Electron micrographs of lungs from an 11-week-old wild-type (A, C, E) and from a periostin-null (B, D, F) mice. Arrowheads indicate vessel walls, and * indicates collagen fibrils. Scale = 500 nm. Abbreviations: T1, type I pneumocyte; T2, type II pneumocyte; FB, fibroblast; CVs, capillary vessels; int, interstitium.

of DNA repair, which DNA is damaged by radical oxygen species produced by bleomycin.[37] Another group reported that C57BL/6 mice transplanted with mesenchymal stem cells from BALB/c mice exhibit improvement in lung inflammation compared with mice without the cell transplantation.[38] In contrast, no significant differences were observed in inflammatory response and collagen production in the lungs of the cell-transplanted mice 7 days post challenge.[38] These results suggest that mesenchymal stem cells from BALB/c

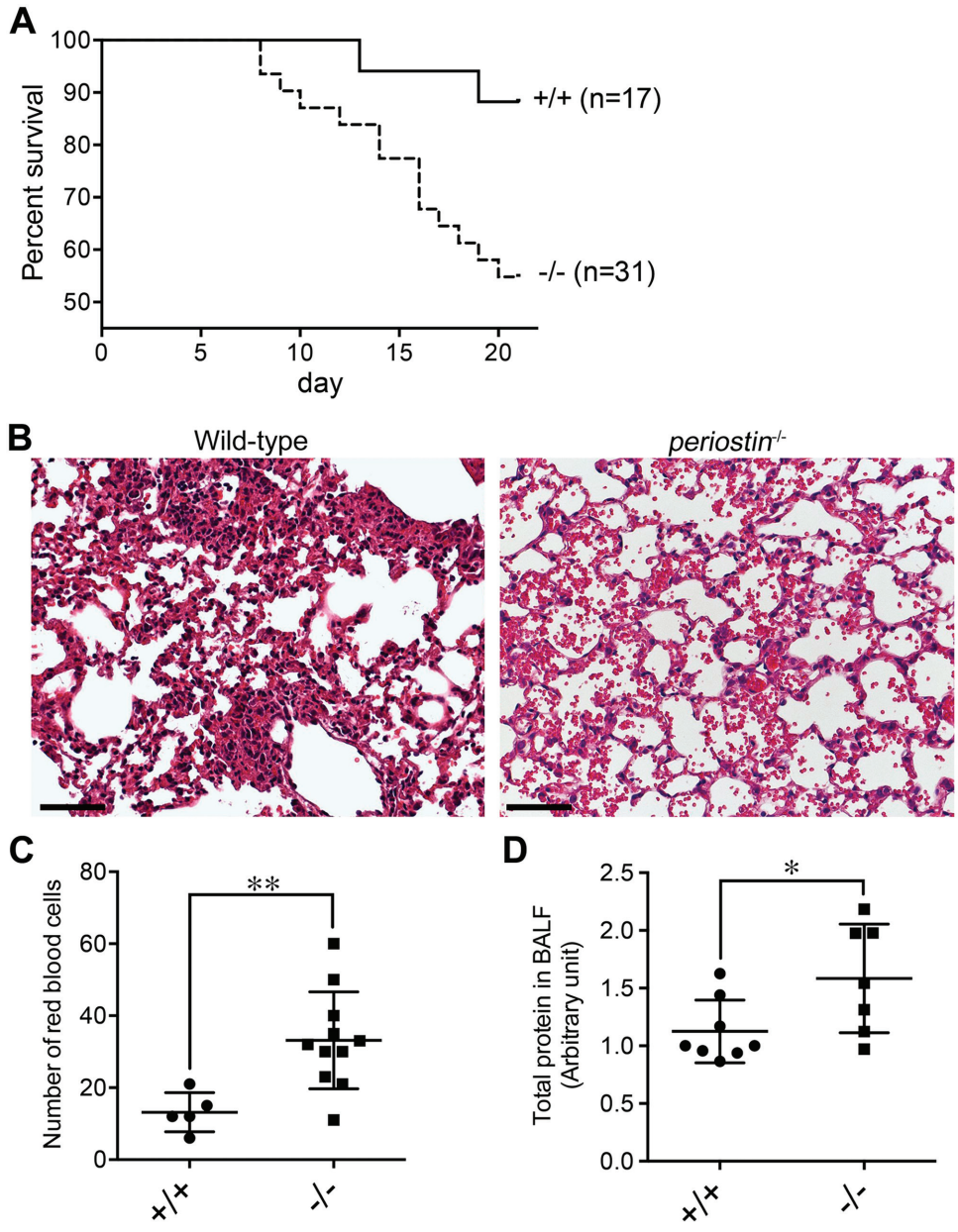

Figure 5. Bleomycin-exposed periostin-null mice show early lethality and blood leakage in their lungs compared with wild-type counterparts. (A) Survival curve of 8-week-old wild-type (+/+; *n*=17) and periostin-null (−/−; *n*=31) mice after the 2.5-U/kg bleomycin administration. The periostin gene is associated with longer survival (p=0.022, log-rank test). (B) Lung histology of 8-week-old wild-type and periostin-null mice at day 7 after the 5.0-U/kg bleomycin administration. The paraffin section was stained with hematoxylin–eosin. (C) Morphometric analysis of erythrocyte concentrations in the lungs of 8-week-old wild-type (+/+; *n*=5) and periostin-null (−/−; *n*=11) mice at day 7 after the 5.0-U/kg bleomycin administration. **p=0.0069. Error bars represent the mean ± SD). (D) Protein concentration of BALF from 8-week-old wild-type (*n*=8) and periostin-null (*n*=7) mice at day 5 after the 5.0-U/kg bleomycin administration. The protein concentration is shown as an arbitrary unit. *p=0.040. Error bars represent the mean ± SD. Scale B = 50 μm. Abbreviation: BALF, bronchoalveolar lavage fluid.

mice improved the symptom of ALI, but not that of PF, in the C57BL/6 strain. Therefore, we employed C57BL/6 background mice with bleomycin in the dose, in which the administration did not cause lethality in wild-type mice.[36,39] Although BALB/c background wild-type and periostin-null mice displayed the same survival rate (about 90%) at the acute phase in the bleomycin administration,[6] we found that C57BL/6 background periostin-null mice exhibited higher lethality than their wild-type counterparts in the case of 2.5

Table 1. Summary of the Roles of Periostin in Bleomycin-Induced Lung Injury From the Three Reports.

	Strain	Intratracheal Administrated Bleomycin (Equivalent Unit, Supplier)	Survival Rate	Cause of Death	Role of Periostin
Uchida et al.[6]	BALB/c; WT (*n*=7) vs. KO (*n*=16)	10 mg/kg (10 U/kg; Nippon Kayaku)	Less than 20% in WT; about 90% in KO (day 28)	Pulmonary fibrosis	Induction of inflammation
Naik et al.[8]	C57BL/6; periostin-neutralizing antibody (injected 10 and 15 days after bleomycin administration, *n*=10 each)	0.05 unit per mouse (about 2 U/kg; Sigma)	40% in control antibody; 100% in neutralizing antibody (day 19)	Pulmonary fibrosis	Fibrosis progression
This study	C57BL/6; WT (*n*=17) vs. KO (*n*=31)	2.5 U/kg (LKT Laboratories)	About 90% in WT; about 55% in KO (day 21)	Alveolar rupture	Increase in ECM stability

WT and KO indicate the wild-type mice and the periostin-null mice, respectively. Abbreviation: ECM, extracellular matrix.

U/kg bleomycin administration. Taken together, our study suggests that periostin strengthens the ECM structure of intact alveolar wall and acts in a protective manner during ALI. On the other hand, the bleomycin-administrated periostin-null mice died during the inflammatory stage (10–20 days after bleomycin administration). Inflammatory response was reported as a cause of death of wild-type mice with BALB/c background, compared with periostin-null mice (Table 1).[6] Further studies on inflammatory response during bleomycin-induced lung injury would be necessary to investigate the cause of death in periostin-null mice with C57BL/6 background.

Periostin has some alternatively spliced variant forms in its carboxyl terminal region, that is, full length, Δb, Δe, and ΔbΔe in mouse periostin.[11,19,35] In this study, we confirmed that the intact lung tissue expressed the ΔbΔe variant (Fig. 1A). Our previous study demonstrated that this variant form recruits fibroblast to the infarcted myocardium via integrin signal activation and that the forced expression of the ΔbΔe variant with adenoviral transduction improved the survival rate of the infarcted periostin-null mice.[11] Another group reported that the periostin Δe variant form is dominantly expressed during idiopathic PF (IPF).[40] These results suggest that periostin in the intact lungs (expressing the ΔbΔe variant form) is different from that in lung fibrosis (expressing the Δe variant form) in terms of function.

The alveolar wall ECM is cross-linked by LOX enzymatic activity, which is responsible for matrix stiffness.[41] The LOX superfamily consists of LOX and LOX-like 1 to 4 (LOXL1–4), and all LOXs are capable of initiating collagen cross-linking.[42,43] Administration of LOX and LOXL1–4 inhibitor β-aminopropionitrile[44–46] to mice downregulates LOX enzymatic activity and consequently leads to a decrease in lung stiffness.[41] Our previous report demonstrated that periostin regulates LOX enzymatic activity, especially LOX and LOXL1, via BMP-1 activation.[30] While LOXL4 is dominantly expressed in the intact lung, LOX and LOXL1 are also weakly observed.[47,48] The collagen cross-linkages in the lung tissues were significantly or tended (without significance) to be decreased in the periostin-null mice compared with those in their wild-type counterpart (Fig. 3). These data suggest that periostin played a role in regulating LOX and LOXL1 enzymatic activity in the lungs. The ECM of the alveolar wall is responsible for tensile strength.[28] The decreased amounts of collagen and cross-linkages in the intact lung of the periostin-null mice might be correlated with the severe ALI in bleomycin-administered periostin-null mice (Figs. 3 and 5).

Intratracheal administration of bleomycin causes alveolar epithelial cell death because of damage due to radical oxygen species generated by bleomycin and increased pulmonary capillary permeability.[7,33] Furthermore, under hypobaric hypoxia especially with exercise[49] and high-pressure ventilation,[50] the intact lungs are injured mechanically and exhibit rupture of the alveolocapillary membrane or a change in the pulmonary permeability. Digesting collagen greatly decreases stiffness,[51] similarly as a decrease in the number of collagen cross-linkages.[42] The lungs of periostin-null mice displayed decreased collagen content and fewer collagen cross-linkages (Fig. 3); therefore, they would have been susceptible to mechanical stress. Thus, periostin-null mice exhibited more severe pulmonary leakages, red blood cell infiltration with alveolar rupture, and hemorrhagic edema than did the wild-type mice (Fig. 5B–D).

The pulmonary edema of periostin-null mice during ALI was obviously more severe than that of the wild-type mice (Fig. 5B). Pulmonary capillary leakage is caused by matrix metalloproteinase (MMP)–mediated disruption of the basement membrane between lung alveoli and pulmonary capillaries.[25,26]

Our previous studies showed that periostin acts as a scaffold of the ECM architecture, for example, interacting with the fibronectin meshwork and basement membrane.[12,14,52] Especially in the epithelial basement membrane between the epidermis and the dermis, periostin increases the transport of fibronectin and laminin 5 gamma 2 chains from keratinocytes to the basement membrane,[14] which reported that the basement membrane without periostin did not affect the keratinocyte proliferation in the intact epidermis. Only during wound healing, they are digested incompletely and that inhibits keratinocyte proliferation.[14] In this study, the permeability of the air–blood barrier in the lungs was an obvious difference between wild-type and periostin-null mice during ALI. These results suggest that the ECM of the lungs of periostin-null mice was more susceptible to bleomycin-induced ALI.

In conclusion, we have reported a lethal phenotype with early and severe disruption of the alveolar–capillary structure in periostin-null mice during ALI induced by 2.5 or 5 U/kg bleomycin. In intact lung tissue, deletion of the periostin gene led to no significant difference in the results of histological or electron microscopic analysis between null and wild-type mice; but the collagen content and number of cross-linkages were decreased in the former. These results suggest that periostin played an important role in maintaining the microstructure and strength of the ECM, which conclusion could not be reached by histological analysis. Further analysis to determine the nature of this microstructural disorder should reveal the molecular function of periostin in lung alveoli.

Acknowledgments

We thank Dr. Takeshi G. Kashima (University of Tokyo, Tokyo, Japan) for critical reading of this manuscript, and Minori Karibe, Yoko Yamamoto, Mamie Suzuki, and Keiko Yamamichi (Tokyo Institute of Technology, Yokohama, Japan) for their technical support.

Author Contributions

HK and TN performed the histological experiments. HK performed pathological experiments. MS quantified the collagen content and cross-linkage. YK and MF supported the histological experiments. HK, TN, and IK analyzed and interpreted the data. HK, TN, IK, and AK designed the research. TN and IK wrote the manuscript.

Competing Interests

The author(s) declared no potential conflicts of interest with respect to the research, authorship, and/or publication of this article.

Funding

The author(s) disclosed receipt of the following financial support for the research, authorship, and/or publication of this article: This work was supported by grants-in-aid for scientific research from the Ministry of Education, Science, Culture, and Sports of Japan (to A.K).

Literature Cited

1. Ware LB, Matthay MA. The acute respiratory distress syndrome. N Engl J Med. 2000;342:1334–49.
2. Raghu G, Collard HR, Egan JJ, Martinez FJ, Behr J, Brown KK, Colby TV, Cordier JF, Flaherty KR, Lasky JA, Lynch DA, Ryu JH, Swigris JJ, Wells AU, Ancochea J, Bouros D, Carvalho C, Costabel U, Ebina M, Hansell DM, Johkoh T, Kim DS, King TE Jr, Kondoh Y, Myers J, Muller NL, Nicholson AG, Richeldi L, Selman M, Dudden RF, Griss BS, Protzko SL, Schunemann HJ; ATS/ERS/JRS/ALAT Committee on Idiopathic Pulmonary Fibrosis. An official ATS/ERS/JRS/ALAT statement: idiopathic pulmonary fibrosis: evidence-based guidelines for diagnosis and management. Am J Respir Crit Care Med. 2011;183:788–824.
3. Kalluri R, Neilson EG. Epithelial-mesenchymal transition and its implications for fibrosis. J Clin Invest. 2003;112:1776–84.
4. Harris WT, Kelly DR, Zhou Y, Wang D, MacEwen M, Hagood JS, Clancy JP, Ambalavanan N, Sorscher EJ. Myofibroblast differentiation and enhanced TGF-B signaling in cystic fibrosis lung disease. PLoS ONE. 2013;8:e70196.
5. Wygrecka M, Dahal BK, Kosanovic D, Petersen F, Taborski B, von Gerlach S, Didiasova M, Zakrzewicz D, Preissner KT, Schermuly RT, Markart P. Mast cells and fibroblasts work in concert to aggravate pulmonary fibrosis: role of transmembrane SCF and the PAR-2/PKC-alpha/Raf-1/p44/42 signaling pathway. Am J Pathol. 2013;182:2094–108.
6. Uchida M, Shiraishi H, Ohta S, Arima K, Taniguchi K, Suzuki S, Okamoto M, Ahlfeld SK, Ohshima K, Kato S, Toda S, Sagara H, Aizawa H, Hoshino T, Conway SJ, Hayashi S, Izuhara K. Periostin, a matricellular protein, plays a role in the induction of chemokines in pulmonary fibrosis. Am J Respir Cell Mol Biol. 2012;46:677–86.
7. Moore BB, Hogaboam CM. Murine models of pulmonary fibrosis. Am J Physiol Lung Cell Mol Physiol. 2008;294:L152–60.
8. Naik PK, Bozyk PD, Bentley JK, Popova AP, Birch CM, Wilke CA, Fry CD, White ES, Sisson TH, Tayob N, Carnemolla B, Orecchia P, Flaherty KR, Hershenson MB, Murray S, Martinez FJ, Moore BB, Investigators C. Periostin promotes fibrosis and predicts progression in patients with idiopathic pulmonary fibrosis. Am J Physiol Lung Cell Mol Physiol. 2012;303:L1046–56.
9. Norris RA, Damon B, Mironov V, Kasyanov V, Ramamurthi A, Moreno-Rodriguez R, Trusk T, Potts JD, Goodwin RL, Davis J, Hoffman S, Wen X, Sugi Y, Kern CB, Mjaatvedt CH, Turner DK, Oka T, Conway SJ, Molkentin JD, Forgacs G, Markwald RR. Periostin

regulates collagen fibrillogenesis and the biomechanical properties of connective tissues. J Cell Biochem. 2007;101:695–711.
10. Oka T, Xu J, Kaiser RA, Melendez J, Hambleton M, Sargent MA, Lorts A, Brunskill EW, Dorn GW 2nd, Conway SJ, Aronow BJ, Robbins J, Molkentin JD. Genetic manipulation of periostin expression reveals a role in cardiac hypertrophy and ventricular remodeling. Circ Res. 2007;101:313–21.
11. Shimazaki M, Nakamura K, Kii I, Kashima T, Amizuka N, Li M, Saito M, Fukuda K, Nishiyama T, Kitajima S, Saga Y, Fukayama M, Sata M, Kudo A. Periostin is essential for cardiac healing after acute myocardial infarction. J Exp Med. 2008;205:295–303.
12. Kii I, Nishiyama T, Li M, Matsumoto K, Saito M, Amizuka N, Kudo A. Incorporation of tenascin-C into the extracellular matrix by periostin underlies an extracellular meshwork architecture. J Biol Chem. 2010;285:2028–39.
13. Kudo A. Periostin in fibrillogenesis for tissue regeneration: periostin actions inside and outside the cell. Cell Mol Life Sci. 2011;68:3201–7.
14. Nishiyama T, Kii I, Kashima TG, Kikuchi Y, Ohazama A, Shimazaki M, Fukayama M, Kudo A. Delayed re-epithelialization in periostin-deficient mice during cutaneous wound healing. PLoS ONE. 2011;6:e18410.
15. Conway SJ, Izuhara K, Kudo Y, Litvin J, Markwald R, Ouyang G, Arron JR, Holweg CT, Kudo A. The role of periostin in tissue remodeling across health and disease. Cell Mol Life Sci. 2014;71:1279–88.
16. Horiuchi K, Amizuka N, Takeshita S, Takamatsu H, Katsuura M, Ozawa H, Toyama Y, Bonewald LF, Kudo A. Identification and characterization of a novel protein, periostin, with restricted expression to periosteum and periodontal ligament and increased expression by transforming growth factor beta. J Bone Miner Res. 1999;14:1239–49.
17. Kii I, Amizuka N, Minqi L, Kitajima S, Saga Y, Kudo A. Periostin is an extracellular matrix protein required for eruption of incisors in mice. Biochem Biophys Res Commun. 2006;342:766–72.
18. Norris RA, Moreno-Rodriguez RA, Sugi Y, Hoffman S, Amos J, Hart MM, Potts JD, Goodwin RL, Markwald RR. Periostin regulates atrioventricular valve maturation. Dev Biol. 2008;316:200–13.
19. Hakuno D, Kimura N, Yoshioka M, Mukai M, Kimura T, Okada Y, Yozu R, Shukunami C, Hiraki Y, Kudo A, Ogawa S, Fukuda K. Periostin advances atherosclerotic and rheumatic cardiac valve degeneration by inducing angiogenesis and MMP production in humans and rodents. J Clin Invest. 2010;120:2292–306.
20. Snider P, Hinton RB, Moreno-Rodriguez RA, Wang J, Rogers R, Lindsley A, Li F, Ingram DA, Menick D, Field L, Firulli AB, Molkentin JD, Markwald R, Conway SJ. Periostin is required for maturation and extracellular matrix stabilization of noncardiomyocyte lineages of the heart. Circ Res. 2008;102:752–60.
21. Wang D, Oparil S, Feng JA, Li P, Perry G, Chen LB, Dai M, John SW, Chen YF. Effects of pressure overload on extracellular matrix expression in the heart of the atrial natriuretic peptide-null mouse. Hypertension. 2003;42:88–95.
22. Fukushima N, Kikuchi Y, Nishiyama T, Kudo A, Fukayama M. Periostin deposition in the stroma of invasive and intraductal neoplasms of the pancreas. Mod Pathol. 2008;21:1044–53.
23. Kikuchi Y, Kashima TG, Nishiyama T, Shimazu K, Morishita Y, Shimazaki M, Kii I, Horie H, Nagai H, Kudo A, Fukayama M. Periostin is expressed in pericryptal fibroblasts and cancer-associated fibroblasts in the colon. J Histochem Cytochem. 2008;56:753–64.
24. Kikuchi Y, Kunita A, Iwata C, Komura D, Nishiyama T, Shimazu K, Takeshita K, Shibahara J, Kii I, Morishita Y, Yashiro M, Hirakawa K, Miyazono K, Kudo A, Fukayama M, Kashima TG. The niche component periostin is produced by cancer-associated fibroblasts, supporting growth of gastric cancer through ERK activation. Am J Pathol. 2014;184:859–70.
25. Davey A, McAuley DF, O'Kane CM. Matrix metalloproteinases in acute lung injury: mediators of injury and drivers of repair. Eur Respir J. 2011;38:959–70.
26. Lee IT, Yang CM. Role of NADPH oxidase/ROS in pro-inflammatory mediators-induced airway and pulmonary diseases. Biochem Pharmacol. 2012;84:581–90.
27. Solomonov I, Talmi-Frank D, Milstein Y, Addadi S, Aloshin A, Sagi I. Introduction of correlative light and airSEM™ microscopy imaging for tissue research under ambient conditions. Sci Rep. 2014;4:5987.
28. Petersen TH, Calle EA, Colehour MB, Niklason LE. Matrix composition and mechanics of decellularized lung scaffolds. Cells Tissues Organs. 2012;195:222–31.
29. Banse X, Sims TJ, Bailey AJ. Mechanical properties of adult vertebral cancellous bone: correlation with collagen intermolecular cross-links. J Bone Miner Res. 2002;17:1621–8.
30. Maruhashi T, Kii I, Saito M, Kudo A. Interaction between periostin and BMP-1 promotes proteolytic activation of lysyl oxidase. J Biol Chem. 2010;285:13294–303.
31. Ahlfeld SK, Gao Y, Wang J, Horgusluoglu E, Bolanis E, Clapp DW, Conway SJ. Periostin downregulation is an early marker of inhibited neonatal murine lung alveolar septation. Birth Defects Res A Clin Mol Teratol. 2013;97:373–85.
32. Matute-Bello G, Frevert CW, Martin TR. Animal models of acute lung injury. Am J Physiol Lung Cell Mol Physiol. 2008;295:L379–99.
33. Tager AM, LaCamera P, Shea BS, Campanella GS, Selman M, Zhao Z, Polosukhin V, Wain J, Karimi-Shah BA, Kim ND, Hart WK, Pardo A, Blackwell TS, Xu Y, Chun J, Luster AD. The lysophosphatidic acid receptor LPA1 links pulmonary fibrosis to lung injury by mediating fibroblast recruitment and vascular leak. Nat Med. 2008;14:45–54.
34. Saito M, Marumo K, Fujii K, Ishioka N. Single-column high-performance liquid chromatographic-fluorescence detection of immature, mature, and senescent cross-links of collagen. Anal Biochem. 1997;253:26–32.

35. Takayama I, Kii I, Kudo A. Expression, purification and characterization of soluble recombinant periostin protein produced by Escherichia coli. J Biochem. 2009;146:713–23.
36. Peng R, Sridhar S, Tyagi G, Phillips JE, Garrido R, Harris P, Burns L, Renteria L, Woods J, Chen L, Allard J, Ravindran P, Bitter H, Liang Z, Hogaboam CM, Kitson C, Budd DC, Fine JS, Bauer CM, Stevenson CS. Bleomycin induces molecular changes directly relevant to idiopathic pulmonary fibrosis: a model for "active" disease. PLoS ONE. 2013;8:e59348.
37. Harrison JH Jr, Hoyt DG, Lazo JS. Acute pulmonary toxicity of bleomycin: DNA scission and matrix protein mRNA levels in bleomycin-sensitive and -resistant strains of mice. Mol Pharmacol. 1989;36:231–38.
38. Ortiz LA, Gambelli F, McBride C, Gaupp D, Baddoo M, Kaminski N, Phinney DG. Mesenchymal stem cell engraftment in lung is enhanced in response to bleomycin exposure and ameliorates its fibrotic effects. Proc Natl Acad Sci U S A. 2003;100:8407–11.
39. Degryse AL, Lawson WE. Progress toward improving animal models for idiopathic pulmonary fibrosis. Am J Med Sci. 2011;341:444–49.
40. Nance T, Smith KS, Anaya V, Richardson R, Ho L, Pala M, Mostafavi S, Battle A, Feghali-Bostwick C, Rosen G, Montgomery SB. Transcriptome analysis reveals differential splicing events in IPF lung tissue. PLoS ONE. 2014;9:e92111.
41. Mammoto A, Mammoto T, Kanapathipillai M, Wing Yung C, Jiang E, Jiang A, Lofgren K, Gee EP, Ingber DE. Control of lung vascular permeability and endotoxin-induced pulmonary oedema by changes in extracellular matrix mechanics. Nat Commun. 2013;4:1759.
42. Maki JM. Lysyl oxidases in mammalian development and certain pathological conditions. Histol Histopathol. 2009;24:651–60.
43. Barker HE, Cox TR, Erler JT. The rationale for targeting the LOX family in cancer. Nat Rev Cancer. 2012;12:540–52.
44. Ito H, Akiyama H, Iguchi H, Iyama K, Miyamoto M, Ohsawa K, Nakamura T. Molecular cloning and biological activity of a novel lysyl oxidase-related gene expressed in cartilage. J Biol Chem. 2001;276:24023–29.
45. Jung ST, Kim MS, Seo JY, Kim HC, Kim Y. Purification of enzymatically active human lysyl oxidase and lysyl oxidase-like protein from Escherichia coli inclusion bodies. Protein Expr Purif. 2003;31:240–46.
46. Rodriguez HM, Vaysberg M, Mikels A, McCauley S, Velayo AC, Garcia C, Smith V. Modulation of lysyl oxidase-like 2 enzymatic activity by an allosteric antibody inhibitor. J Biol Chem. 285:20964–74.
47. Asuncion L, Fogelgren B, Fong KS, Fong SF, Kim Y, Csiszar K. A novel human lysyl oxidase-like gene (LOXL4) on chromosome 10q24 has an altered scavenger receptor cysteine rich domain. Matrix Biol. 2001;20:487–91.
48. Nave AH, Mizikova I, Niess G, Steenbock H, Reichenberger F, Talavera ML, Veit F, Herold S, Mayer K, Vadasz I, Weissmann N, Seeger W, Brinckmann J, Morty RE. Lysyl oxidases play a causal role in vascular remodeling in clinical and experimental pulmonary arterial hypertension. Arterioscler Thromb Vasc Biol. 2014;34:1446–58.
49. Bai C, She J, Goolaerts A, Song Y, Shen C, Shen J, Hong Q. Stress failure plays a major role in the development of high-altitude pulmonary oedema in rats. Eur Respir J. 2010;35:584–91.
50. Koeppen M, Eckle T, Eltzschig HK. Pressure controlled ventilation to induce acute lung injury in mice. J Vis Exp. 2011;51:e2525.
51. Yuan H, Kononov S, Cavalcante FS, Lutchen KR, Ingenito EP, Suki B. Effects of collagenase and elastase on the mechanical properties of lung tissue strips. J Appl Physiol (1985).2000;89:3–14.
52. Kii I, Nishiyama T, Kudo A. Periostin promotes secretion of fibronectin from the endoplasmic reticulum. Biochem Biophys Res Commun. 2016;470:888–93.